Zeitschrift für Kristallographie, Bd. 137, S. 86—105 (1973)

Four new structure refinements of olivine

By **H.-R. Wenk**

Department of Geology and Geophysics and Space Sciences Laboratory
University of California at Berkeley

and **K. N. Raymond**

Department of Chemistry, University of California at Berkeley

(Received 2 February 1972)

Auszug

Mg/Fe-Ordnung in Olivin wurde von Finger (1969/70) auf Grund von Röntgendaten vorgeschlagen und mit Mössbauer-Spektren (Bush *et al.*, 1970) bewiesen. Neue Strukturverfeinerungen an vier magnesiumreichen Olivinen ergaben Werte für Extinktionskoeffizienten, Atomlagen, anisotrope Temperaturfaktoren, Mg/Fe-Verteilung und formale Ladungen mit zwei- bis zehnmal besserer Auflösung als bisher. Die Parameter wurden mit der Methode der kleinsten Quadrate von Röntgendaten verfeinert unter Berücksichtigung der Einschränkungen durch chemische Zusammensetzung und elektrostatische Neutralität auf die Ableitungen. *R*-Werte liegen zwischen 2% und 3%. Mondproben zeigen signifikante (20 Standardabweichungen) Ordnung von Fe auf der kleineren M(1)-Lage [52% Fe auf M(1), 48% auf M(2)], metamorphe Forsterite sind grundsätzlich ungeordnet. Formale Ladungen wurden bestimmt: Fe,Mg $= +0{,}3$; Si $= +0.2$ und O $= -0{,}2$. Der Extinktionskoeffizient, ein empfindliches Maß für strukturelle Defekte, ist viel kleiner für Proben aus dem Mondstaub, die Strahlungsschäden und Wirkungen von Stoßwellendeformation zeigen, als für die metamorphen Forsterite. Mittlere M(1)—O- und M(2)—O-Abstände nehmen linear mit dem Fe/(Fe + Mg)-Quotienten zu.

Abstract

Mg/Fe order in olivine has been suggested from x-ray data (Finger, 1969/70) and proven with Mössbauer spectra (Bush *et al.*, 1970). New structure refinements on four magnesium-rich olivines give two to ten times improved values for extinction coefficients, atomic positions, anisotropic temperature factors, site occupancies, and formal charges. The parameters have been refined from x-ray data by least-squares methods imposing proper constraints of chemical composition and electrostatic neutrality on derivatives. *R* factors range between 2 and 3%. Lunar samples show significant (twenty standard deviations) order of Fe on the smaller M(1) site [52% Fe on M(1), 48% Fe on M(2)], metamorphic forsterites are essentially disordered. Formal charges have been determined: Fe,Mg = + 0.3, Si = + 0.2, O = −0.2. The extinction coefficient, a sensitive measure for structural defects, is much lower for specimens from lunar dust, which show radiation damage and possible effects of shock deformation. Mean M(1)—O and M(2)—O distances increase linearly with Fe/(Fe + Mg).

Introduction

Bragg and Brown (1926) determined the basic structure of olivine and found hexagonal close packing of oxygen with Mg and Fe occupying half of the distorted octahedral interstices [the M(1) and M(2) sites], and Si occupying one-eighth of the tetrahedral interstices [the T site], see Fig. 1. Structures of olivines of different compositions have been refined, with emphasis on the determination of structural variations in this Mg-Fe solid solution series. Until recently, however, no deviations from ideal substitution have been found (Belov *et al.*, 1951; Born, 1964; Hanke and Zemann, 1963; Hanke, 1963; Birle *et al.*, 1968). Eliseev (1958) reported deviations of the lattice parameters from Vegard's rule in the fayalite-forsterite solid

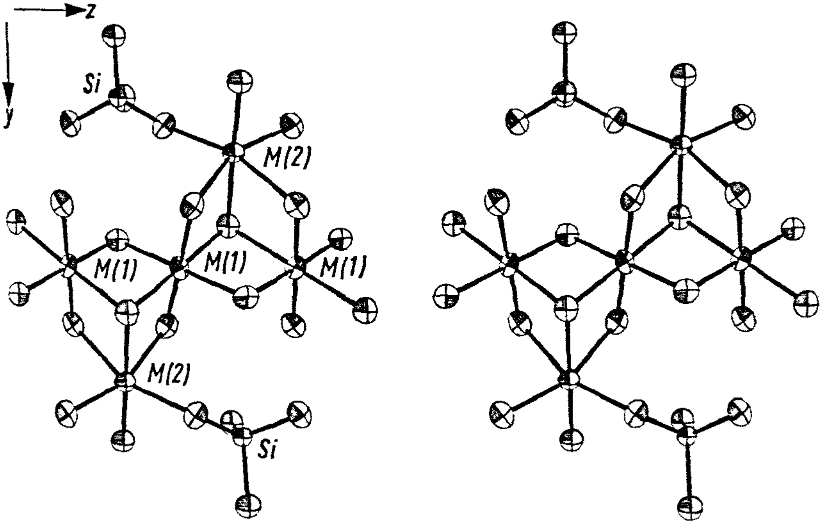

Fig. 1. Stereoscopic pair of drawings showing the crystal structure of olivine (Yosemite forsterite). The ellipsoids represent 99% probability contours of thermal motion. z axis is horizontal, y axis vertical, view is along x

solution series, which was probably based on inaccurate chemical data. GHOSE (1962) predicted that Fe would preferentially occupy the larger M(2) site, in analogy to orthopyroxenes. These suggestions and the fact that in isostructural compounds like monticellite, $CaMgSiO_4$ (ONKEN, 1965), and glaucochroite, $CaMnSiO_4$ (CARON *et al.*, 1965), the cations are ordered encouraged other investigators to continue the search for order in olivines. It has been the stimulus of the moon that has led several crystallographers independently to refine structures of lunar olivines to determine if the Fe/Mg distribution can be used as an indicator for the geological history of these important minerals, which occur in many different rocks and which have been formed under very different geological conditions.

Partial order was first suggested from spectroscopic measurements (BURNS, 1969; BUSH *et al.*, 1970) but the results were not conclusive (BURNS, 1970). The latest development of x-ray single-crystal diffractometers has improved the quality of x-ray data and thus enhances the resolution of a standard crystal-structure refinement. It becomes possible to determine electron densities in fractions of an electron. The refinements of FINGER (1969/70, 1971) suggest preference of Fe on the M(1) site in igneous olivines, with deviations from disorder of a few standard deviations. BROWN (1971) describes small order, which they think is insignificant. In their high-temperature experiments they find an increasing distortion of the M(1) site with increasing temperature. With this background in mind, and with the need to obtain data on lunar crystals, the present investigation has been started. The aim was to push the resolution of a refinement to its limits to determine if order in igneous olivines is real. This paper consists of two equally important parts: The first part discusses in some detail the influence of more than one dependent and independent constraint of the occupancy factors on the derivatives in the least-squares refinement. So far, only a single constraint has been taken into account in the refinement of mineral structures (FINGER, 1967). The second part presents the results of four crystal-structure refinements and tries to demonstrate that these results are not experimental artifacts. FINGER's results have been confirmed. There exists small but significant order in chemically intermediate olivines. Yet it has not been possible to resolve the olivine controversy (the question whether the thermal history affects the Fe/Mg distribution), and more structural work should be done on geologically well-defined olivines.

Experimental procedure

Data collection

Small crystals (0.1—0.2 mm) of isometric shape were selected from various rock specimens; two are metamorphic forsterites and two are intermediate (Fa 30) olivines from lunar basalt. Specifications are given in Table 1. The crystals were first checked on a precession camera for space group, domain structure, and asterism. For all of them, the space group *Pbnm* was determined. No extra reflections have been observed (ELISEEV, 1958). Then the crystals were oriented on a computer-controlled Picker diffractometer. From the positions of twelve reflections, the lattice constants and the orientation angles were refined by least squares (Table 2). They agree closely (Fig. 2), but not perfectly, with the determinative curves of YODER and SAHAMA (1957), JAMBOR and SMITH (1964), and JAHANBAGLOO (1969). Data were collected by the θ-2θ scan technique up to Bragg angles of 100° using monochromatic Mo$K\alpha$ radiation, with highly oriented graphite used as the monochromator crystal. The 2θ scan width was $1.4° + \Delta 2\theta$ where $\Delta 2\theta$ is the distance between the calculated maxima for the $K_{\alpha 1}$ and $K_{\alpha 2}$ peaks. The scanning rate was 1 degree per minute with 10-second stationary background counts on either side of the scan. Standard deviations of individual reflections were determined from

Table 1. *General information about the olivines investegated*

Specimen number	Source	Mineralogical description
103—481	Yosemite 1-1/2 miles southwest May Lake	brucite-forsterite-humite-spinel-calcite marble
Sci 59	Bergell Alps Road cut Casalic 1160 m, Bondo-Ceresc	amphibole-orthopyroxene-chlorite olivinite, recrystallized
12070—12.4	Oceanus Procellarum Apollo 12	fine lunar dust, single crystal
10085	Mare Tranquillitatis Apollo 11	coarse fines, plagioclase-pyroxene-ilmenite-olivine basalt

Table 2. *Lattice constants of olivines (Pbnm setting)*

Lattice constants	Yosemite 103—481	Bergell Alps Sci 59	Oceanus Procellarum Apollo 12 12070—12.4	Mare Tranquillitatis Apollo 11 10085
a	4.7533(5)[1]	4.7623(4)	4.7748(5)	4.7768(6) Å
b	10.1972(7)	10.2284(11)	10.2798(16)	10.2943(16) Å
c	5.9821(3)	5.9942(6)	6.0087(9)	6.0174(9) Å

[1] In this and the following tables standard deviations in the least significant digits are given in parentheses.

Table 3. *X-ray data collection*

Parameter data	Yosemite 103—481	Bergell Alps Sci 59	Oceanus Procellarum Apollo 12 12070-12.4	Mare Tranquillitatis Apollo 11 10085
Crystal size	0.15 × 0.15 × 0.15mm	0.15 × 0.10 × 0.10mm	0.2 × 0.15 × 0.1mm	0.3 × 0.2 × 0.2mm
Linear absorption coefficient μ	11	19	40	45 cm^{-1}
Total number of observations	1427	3644	2349	3161
Number of independent observations	1125	1797	1321	2029
Number of independent reflections used in refinement ($F_o^2 > 3\sigma$)	783	851	882	1459
R factor (all data)	0.023	0.022	0.022	0.022
Weighted R (all data)	0.032	0.026	0.029	0.032

counting statistics of integrated count and background (DUESLER and RAYMOND, 1971). An additional error of 3% of the net intensity was added to the standard deviation to avoid overweighting of intense reflections. The raw intensities were corrected for Lorentz and polarization effects. An absorption correction was not found to be necessary because intensities of equivalent reflections were not significantly different. Intensities of equivalent reflections were averaged. Systematic extinctions were rejected. A new standard deviation of the averaged intensity was calculated. The larger one (counting statistic averaging) was used as weight in the least-squares refinement. More

Table 4. *Chemical composition of olivines*
(microprobe analyses)

	Yosemite 103–481	Bergell Alps Sci 59	Oceanus Procellarum Apollo 12 12070-12.4	Mare Tranquillitatis Apollo 11 10085[1]
Weight percent				
SiO_2	42.21%	~37.79%	37.10%	36.88%
FeO	1.21	9.25	27.53	26.37
TiO_2	—			
MnO	0.29	0	0	0
NiO	traces	0.74	0.37	0
MgO	56.03	49.30	34.17	35.95
CaO	0.06	0.02	0.35	0.36
Na_2O	—			
Total	99.80	97.1	99.52	99.56
Formula used in refinement				
Fe	0.012	0.099	0.319	0.300[2]
Mn	0.003	—	—	—
Ni	0 } 1	0.008	0.004	0
Mg	0.985	0.893	0.672	0.695
Ca	< 0.001	0	0.005	0.005
Si	0.5	0.5	0.5	0.5
O	2	2	2	2
Refined formula from x-ray data				
Fe				0.358(5)
Mg				0.637
Ca				0.005

[1] Chemical analysis done on different crystal from the same rock.
[2] Later replaced by formula below.

information about the specimens data collection and data processing is given in Table 3. After the data collection, the crystals were chemically analyzed with the microprobe (Table 4). During this procdeure the Apollo 11 crystal was lost and the analysis was done on another crystal from the same rock. This crystal apparently did not have an identical composition, which was readily seen in aberrant electrical charges for Si. The final Fe/Mg ratio was therefore refined from the x-ray data.

Least-squares refinement

The refinement of the structure was done with a modified version of the Busing-Levy least-squares program (Busing *et al.*, 1962). Atomic scattering factors were interpolated from the table of Cromer and Mann (1968). Real and imaginary anomalous scattering factors were used for Fe (Cromer, 1965). Several assumptions for the structure model were made: a) there are no vacancies; b) traces of Mn and Ni are closely related to iron, and the atomic scattering factors were adjusted accordingly; c) all Ca is on the M(2) site in analogy to monticellite; d) the overall electrical charge is zero; e) all oxygen has equal charge; f) the degree of ionization of Fe and Mg is equal; g) atomic scattering factors for neutral atoms were used. All refined parameters are relatively insensitive to each of these assumptions. Errors in the chemical analysis (Fe/Mg ratio) are mainly expressed in the refined electrical charge and not in the Fe/Mg distribution. The 44 positional, thermal and scale parameters which were refined imposing proper constraints on the derivatives are: a) atomic coordinates of M(2), Si, O(1), O(2), and O(3); b) anisotropic temperature factors for all atoms; c) scale factors for Fe(1), Fe(2), and Si to calculate the Fe/Mg distribution and an approximated ionic charge; d) an overall isotropic extinction factor (Zachariasen, 1968). After a few cycles the refinement converged with R values of 2–3%.

The least-squares refinement of site occupancies has to take into account constraints imposed by the chemical composition, the lattice geometry, and overall electrostatic neutrality. If many independent and correlated constraints are acting, then the effect on the derivatives is no longer trivial. We think that the best way to explain the procedure to the reader is to specify explicitely for each refinement all the variables and constraints. This specification, which permits an evaluation of the refinement procedure, is done most compactly in matrix notation. Raymond (1972) derived the formal solution of the general problem. A crystal has n atoms, and each atom has a multiplicity factor a_i. We cannot refine all of these multiplicity factors because of constraints. If there are n atoms and m linear equations of constraint, then there are only $k = n - m$ independent variables, V_k. We form a square matrix, Q, by combining independent variables with the constraints. In the following discussion, variables and constraints are specified for each crystal. For the *Yosemite forsterite* with very little Fe, the refinement has been done on the basis of the formula (Mg,Fe)SiO_4 with six atoms [M(1), M(2), Si, O(1), O(2), O(3)]. Occupancies of M(1), M(2), and Si were refined, thus the matrix becomes

$$Q = \begin{bmatrix} 1 & 0 & 0 & 0 & 0 & 0 \\ 0 & 1 & 0 & 0 & 0 & 0 \\ 0 & 0 & 1 & 0 & 0 & 0 \\ 12.303 & 12.203 & 14 & 8 & 8 & 8 \\ 0 & 0 & 0 & 1 & -1 & 0 \\ 0 & 0 & 0 & 2 & 0 & -1 \end{bmatrix} \begin{bmatrix} a_{(\mathrm{M})1} \\ a_{(\mathrm{M})2} \\ a_{\mathrm{Si}} \\ a_{(\mathrm{O})1} \\ a_{(\mathrm{O})2} \\ a_{(\mathrm{O})3} \end{bmatrix} = \begin{bmatrix} V_1 \\ V_2 \\ V_3 \\ C_1\,[35.203] \\ C_2\,[0] \\ C_3\,[0] \end{bmatrix}$$

The first constraint, C_1, ensures that electrostatic neutrality is maintained. The number of electrons of the neutral metal atom (Mg, corrected for traces of Fe and Mn) is 12.203. Constraints C_2 and C_3 impose equal occupancy on the oxygen sites. From the refined occupancies, an approximate formal electrical charge, q, can be calculated:

$$q = \frac{Z(a_i^0 - a_i)}{a_i},$$

where a_i^0 is the occupancy in the chemical formula, and a_i is the refined occupancy. The atomic number of the element is Z. This refinement of the charge from a constant scale factor is not strictly true because the scattering-factor curve for an ionized atom is not proportional to that of a neutral atom. The two curves differ mostly at low diffraction angles and almost coincide at high angles. But as scale factors are mainly determined by low-angle reflections and because charges were very small, it was found sufficient to use scattering-factor tables for neutral atoms and to refine a scale factor. It would be more accurate to interpolate a new scattering-factor table after each cycle of the refinement. Yet this raw treatment of charges is certainly better than ignoring them and produces very reasonable results. Notice that, due to the refinement of the electrical charge, the occupancy of oxygen, a_{O}, in the second and third constraint equations is not constant.

In the case of the *Bergell olivine* (Sci 59) the relation is more complicated. There is now sufficient Fe to separate the M sites into an Fe and an Mg contribution. Traces of other transition elements (e.g. Ni, Mn) are combined with the chemically similar Fe. The formula is $Fe_{0.107}Mg_{0.893}SiO_4$ with eight atoms [Fe(1), Fe(2), Si, Mg(1), Mg(2), O(1), O(2), O(4)]. Occupancies of Fe(1), Fe(2), and Si were refined and two additional constraints were introduced. The first constraint imposes equal occupancy of M(1) and M(2), and C_2 introduces the Fe/Mg ratio obtained from the chemical analysis. Formal charges, q, were taken into account. The equations are no longer strictly linear and were reset for q after every cycle in the refinement.

$$Q = \begin{bmatrix} 1 & 0 & 0 & 0 & 0 & 0 & 0 & 0 \\ 0 & 1 & 0 & 0 & 0 & 0 & 0 & 0 \\ 0 & 0 & 1 & 0 & 0 & 0 & 0 & 0 \\ b_1 & -b_1 & 0 & b_2 & -b_2 & 0 & 0 & 0 \\ b_1 & b_1 & 0 & -b_2\cdot\frac{\mathrm{Fe}}{\mathrm{Mg}} & -b_2\cdot\frac{\mathrm{Fe}}{\mathrm{Mg}} & 0 & 0 & 0 \\ 26.134 & 26.134 & 14 & 12.0 & 12.0 & 8 & 8 & 8 \\ 0 & 0 & 0 & 0 & 0 & -1 & 1 & 0 \\ 0 & 0 & 0 & 0 & 0 & -2 & 0 & 1 \end{bmatrix} \begin{bmatrix} a_{\mathrm{Fe(1)}} \\ a_{\mathrm{Fe(2)}} \\ a_{\mathrm{Si}} \\ a_{\mathrm{Mg(1)}} \\ a_{\mathrm{Mg(2)}} \\ a_{\mathrm{O(1)}} \\ a_{\mathrm{O(2)}} \\ a_{\mathrm{O(3)}} \end{bmatrix} = \begin{bmatrix} V_1 \\ V_2 \\ V_3 \\ C_1\,[0] \\ C_2\,[0] \\ C_3\,[36.50] \\ C_4\,[0] \\ C_5\,[0] \end{bmatrix}$$

where $b_1 = \frac{26.134 + q}{26.134}$, $b_2 = \frac{12.0 + q}{12.0}$, and $\mathrm{Fe/Mg} = 0.1198$.

The lunar samples *Apollo 11* and *Apollo 12* contain enough Ca to treat it as a separate atom. In the isostructural monticellite ($CaMgSiO_4$), Ca is ordered on the M(2) site (ONKEN, 1965) and it was placed there by analogy. For Apollo 11 the formula is $Fe_{0.300}Mg_{0.695}Ca_{0.004}SiO_4$; and for Apollo 12 it is $Fe_{0.323}Mg_{0.672}Ca_{0.004}SiO_4$ with nine atoms: the same independent variables were used as before.

$$\begin{bmatrix} 1 & 0 & 0 & 0 & 0 & 0 & 0 & 0 & 0 \\ 0 & 1 & 0 & 0 & 0 & 0 & 0 & 0 & 0 \\ 0 & 0 & 1 & 0 & 0 & 0 & 0 & 0 & 0 \\ +b_1 & -b_1 & 0 & b_2 & -b_2 & -1 & 0 & 0 & 0 \\ b_1 & b_1 & 0 & -b_2\cdot\frac{\mathrm{Fe}}{\mathrm{Mg}} & -b_2\cdot\frac{\mathrm{Fe}}{\mathrm{Mg}} & 0 & 0 & 0 & 0 \\ 0 & 0 & 0 & 0 & 0 & 1 & 0 & 0 & 0 \\ \substack{26.0(11) \\ 26.015(12)} & \substack{26.0 \\ 26.015} & 14 & 12 & 12 & 20 & 8 & 8 & 8 \\ 0 & 0 & 0 & 0 & 0 & 0 & \bar{1} & 1 & 0 \\ 0 & 0 & 0 & 0 & 0 & 0 & \bar{2} & 0 & 1 \end{bmatrix} \begin{bmatrix} a_{\mathrm{Fe(1)}} \\ a_{\mathrm{Fe(2)}} \\ a_{\mathrm{S}} \\ a_{\mathrm{Mg(1)}} \\ a_{\mathrm{Mg(2)}} \\ a_{\mathrm{Ca(2)}} \\ a_{\mathrm{O(1)}} \\ a_{\mathrm{O(2)}} \\ a_{\mathrm{O(3)}} \end{bmatrix} = \begin{bmatrix} V_1 \\ V_2 \\ V_3 \\ C_1\ [0] \\ C_2\ [0] \\ C_3\ [0.005] \\ C_4 \substack{[39.240] \\ [39.566]} \\ C_5\ [0] \\ C_6\ [0] \end{bmatrix}$$

with $b_1 = \frac{26 + q}{26}$, $b_2 = \frac{12 + q}{12}$, and Fe/Mg = 0.4317 for Apollo 11 and $b_1 = \frac{26.015 + q}{26.015}$, $b_2 = \frac{12 + q}{12}$, and Fe/Mg = 0.4927 for Apollo 12. The refinements were done weighing the reflections indirectly proportional to their standard deviation. To check the quality of the data, the final cycles have also been done with unit weights for all reflections. The results agreed within one or two standard deviations.

Table 5. *Atomic parameters of olivine*

	Yosemite 103—481	Bergell Alps Sci 59	Oceanus Procellarum Apollo 12 12070-12.4	Mare Tranquillitatis Apollo 11 10085
M(1)				
$x = y = z = 0$				
M(2)				
x	0.99119(10)	0.98968(8)	0.98765(7)	0.98724(5)
y	0.27744(4)	0.27772(4)	0.27821(3)	0.27842(2)
$z = 1/4$				
Si				
x	0.42625(7)	0.42681(7)	0.42752(7)	0.42786(5)
y	0.09409(4)	0.09443(4)	0.09521(4)	0.09535(3)
$z = 1/4$				
O(1)				
x	0.76557(20)	0.76589(18)	0.76603(19)	0.76645(13)
y	0.09144(9)	0.09148(9)	0.09185(9)	0.09211(7)
$z = 1/4$				
O(2)				
x	0.22163(20)	0.22066(19)	0.21720(20)	0.21690(14)
y	0.44721(8)	0.44767(8)	0.44882(8)	0.44930(6)
$z = 1/4$				
O(3)				
x	0.27723(12)	0.27838(13)	0.28034(13)	0.28122(9)
y	0.16311(6)	0.16333(6)	0.16381(6)	0.16406(5)
z	0.03315(11)	0.03329(10)	0.03431(10)	0.03422(8)

Table 6. *Site occupancies and apparent charges of olivines*

	Yosemite 103—481	Bergell Alps Sci 59	Oceanus Procellarum Apollo 12 12070-12.4	Mare Tranquillitatis Apollo 11 10085
Occupancies				
M(1)				
Fe	0.006(3)	0.0526(6)	0.1672(6)	0.1871(7)
Mg	0.494	0.4474	0.3328	0.3129
M(2)				
Fe	0.009(4)	0.0541(6)	0.1558(4)	0.1709(7)
Mg	0.491	0.4459	0.3392	0.3241
Ca	—	—	0.005	0.005
K_D	[0.66(20)]	0.969(24)	1.096(10)	1.134(11)
Charges per atom				
M(1) = M(2)	+ 0.33(3)	+ 0.22(3)	0.34(4)	0.13(5)
Si	+ 0.27(3)	+ 0.20(8)	+ 0.03(3)	0.14(3)
O(1)=O(2)=O(3)	−0.23	−0.15	−0.18	−0.10
Extinction coefficient	$0.90(4) \cdot 10^{-6}$	$2.94(11) \cdot 10^{-6}$	$0.15(4) \cdot 10^{-6}$	$0.27(2) \cdot 10^{-6}$

Table 7. *Thermal parameters of olivines* ($\beta \times 10^5$)
(Temperature factors are of the form $\exp\left[-(\beta_{11}h^2 + \beta_{22}k^2 + \beta_{33}l^2 + 2\beta_{12}hk + 2\beta_{13}hl + 2\beta_{23}kl)\right]$)

	Yosemite 103—481	Bergell Alps Sci 59	Oceanus Procellarum Apollo 12 12070-12.4	Mare Tranquillitatis Apollo 11 10085
M(1)				
β_{11}	333(15)	287(12)	498(10)	417(6)
β_{22}	140(3)	110(3)	162(3)	147(2)
β_{33}	316(10)	214(8)	204(7)	347(4)
β_{12}	− 9(5)	0(5)	− 4(3)	− 5(2)
β_{13}	−43(9)	−40(7)	−36(5)	−45(3)
β_{23}	−34(5)	−36(4)	−41(3)	−41(2)
M(2)				
β_{11}	418(17)	470(14)	692(13)	585(7)
β_{22}	99(4)	69(3)	106(2)	94(1)
β_{33}	375(11)	269(8)	240(7)	365(4)
β_{12}	9(6)	2(5)	14(4)	2(2)
$\beta_{13} = \beta_{23} = 0$				

Table 7. *(Continued)*

	Yosemite 103–481	Bergell Alps Sci. 59	Oceanus Procellarum Apollo 12 12070-12.4	Mare Tranquillitatis Apollo 11 10085
Si				
β_{11}	178(12)	133(11)	340(11)	257(7)
β_{22}	88(3)	56(2)	99(2)	89(2)
β_{33}	284(8)	179(6)	172(7)	301(5)
β_{12}	2(4)	4(4)	9(4)	13(2)
$\beta_{13} = \beta_{23} = 0$				
O(1)				
β_{11}	389(26)	238(24)	493(26)	369(14)
β_{22}	164(7)	145(6)	179(6)	172(3)
β_{33}	436(18)	329(16)	285(15)	431(11)
β_{12}	5(10)	11(11)	7(10)	15(6)
$\beta_{13} = \beta_{23} = 0$				
O(2)				
β_{11}	530(27)	501(27)	699(27)	619(17)
β_{22}	124(6)	84(6)	114(5)	103(3)
β_{33}	466(18)	326(16)	358(15)	463(11)
β_{12}	2(11)	10(10)	4(11)	–12(6)
$\beta_{13} = \beta_{23} = 0$				
O(3)				
β_{11}	514(19)	445(17)	634(19)	576(12)
β_{22}	172(5)	127(4)	182(4)	161(3)
β_{33}	445(13)	326(11)	320(11)	445(8)
β_{12}	1(8)	24(7)	13(7)	25(5)
β_{13}	–22(13)	–15(12)	–25(11)	–10(8)
β_{23}	45(6)	54(5)	70(5)	66(4)

Results

The refined parameters are listed in Tables 5, 6, and 7. We will discuss briefly the significance and importance of these results. Standard deviations are especially low for the Apollo 11 olivine, where 1459 independent reflections have been used in the refinement.

Atomic positions

From atomic positions selected interatomic distances were calculated (Table 8), and the important mean M(1)–O and M(2)–O distances are plotted in Fig. 2 as a function of the fayalite content.

Results of previous work are included. The new data show that both distances increase linearly with iron content. M(2)—O is about 0.03 Å larger than M(1)—O, and one might expect M(2) to be preferentially occupied by Fe, although the difference in size is quite small. A linear dependence is a reasonable physical assumption for an ideal ionic substitution. The strictly linear relation between calculated M—O distances and fayalite content within two standard deviations as documented by the four new data points is a good indication, although not a definite proof, that the standard deviation computed in the least-squares program is meaningful, and that the dependence, in fact, is linear. If either one of these assumptions were not true, it would be

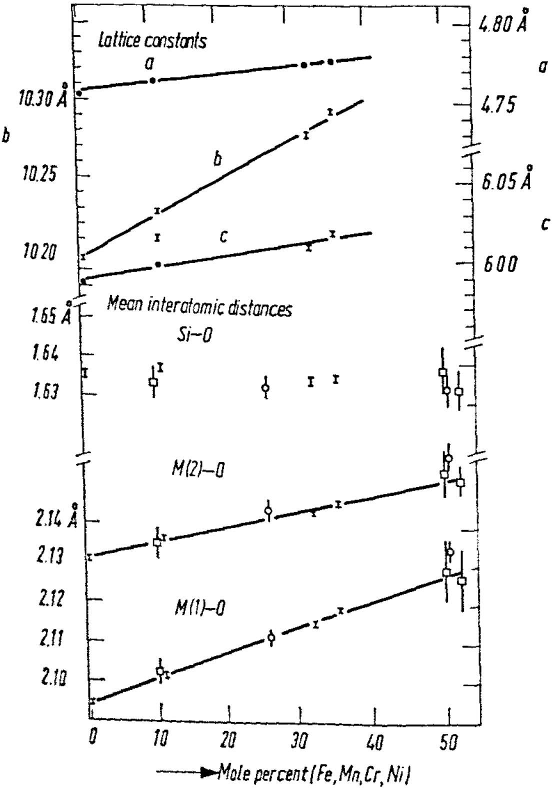

Fig. 2. Lattice constants and selected mean interatomic distances of olivines as a function of the iron content (error bars are rounded to 1—2 sigmas). □ Birle *et al.* (1968), ○ Finger (1969/70), ● and ɪ this paper

Table 8. *Selected interatomic distances of olivines*

	Yosemite 103—481	Bergell Alps Sci 59	Oceanus Procellarum Apollo 12 12070-12.4	Mare Tranquillitatis Apollo 11 10085
		Si tetrahedron		
1 Si—O(1)	1.6131(10) Å	1.6150(9) Å	1.6167(10) Å	1.6177(7) Å
1 O(2)	1.6545(9)	1.6572(9)	1.6559(10)	1.6549(7)
2 O(3)	1.6370(7)	1.6382(7)	1.6343(6)	1.6361(5)
mean	1.6354(8)	1.6372(8)	1.6353(7)	1.6362(6)
1 O(1)—O(2)	2.7434(13)	2.7445(13)	2.7360(14)	2.7371(20)
—O(3)	2.7577(10)	2.7600(6)	2.7577(10)	2.7580(8)
1 O(2)—O(3)[a]	2.5553(10)	2.5599(10)	2.5620(10)	2.5639(8)
1 O(3)—O(3)[a]	2.5945(13)	2.5980(13)	2.5920(12)	2.5968(11)
		M(1) octahedron		
2 M(1)—O(1)	2.0851(6)	2.0891(6)	2.0967(7)	2.0992(5)
2 —O(2)	2.0681(6)	2.0741(6)	2.0873(7)	2.0891(5)
2 —O(3)	2.1313(6)	2.1420(6)	2.1610(7)	2.1678(5)
mean	2.0948(6)	2.1017(6)	2.1150(7)	2.1187(5)
2 O(1)—O(2)[b]	2.847(10)	2.854(10)	2.872(10)	2.873(8)
2 —O(2)	3.0241(2)	3.0314(4)	3.0423(5)	3.0479(5)
2 —O(3)[b]	2.8516(11)	2.8608(10)	2.8735(10)	2.8777(8)
2 —O(3)	3.106(10)	3.118(10)	3.218(10)	3.151(8)
2 O(2)—O(3)[a]	2.5553(10)	2.5599(10)	2.5620(10)	2.5639(8)
—O(3)	3.3330(9)	3.3507(10)	3.3896(11)	3.3990(8)
		M(2) octahedron		
1 M(2)—O(1)	2.1788(10)	2.1829(10)	2.1886(11)	2.1889(8)
1 —O(2)	2.0487(10)	2.0571(9)	2.0682(10)	2.0731(7)
2 —O(3)	2.2114(8)	2.2241(7)	2.2396(7)	2.2459(6)
2 —O(3)	2.0666(7)	2.0639(7)	2.0624(7)	2.0601(5)
mean	2.1306(7)	2.1360(7)	2.1435(7)	2.1456(6)
2 O(1)—O(3)[b]	2.8516(11)	2.8608(10)	2.8735(10)	2.8777(8)
2 —O(3)	3.0226(10)	3.0293(10)	3.0384(10)	3.0382(8)
2 O(2)—O(3)	3.1852(10)	3.1972(10)	3.2179(11)	3.2235(9)
2 —O(3)	2.9320(9)	2.9341(9)	2.9343(10)	2.9357(7)
1 O(3)—O(3)[a]	2.5945(13)	2.5980(13)	2.5920(12)	2.5968(11)
2 —O(3)	3.3876(13)	3.3962(13)	3.4167(13)	3.4206(11)
2 —O(3)	2.9910(8)	2.9955(8)	3.0016(8)	3.0008(7)

[a] Edges shared between tetrahedron and octahedron.

[b] Edges shared between octahedra.

highly improbable that the error bars fall exactly on a straight line of all four data points. If the errors were artificially low, we would expect error bars to scatter outside the straight line in Fig. 3, as would be the case if smaller errors were assigned to the data points of Birle *et al.* (1968) and Finger (1969/70).

Temperature factor

Anisotropic temperature factors have been refined for all atoms, imposing proper symmetry constraints. Numerical values are listed in Table 7. They are relatively small, larger for the lunar olivines than for the terrestrial forsterites. We attribute this to some structural defect, such as domain texture in the lunar crystals. Figure 1, where 99% probability contours are drawn for the Yosemite forsterite, shows a moderate anisotropy. Table 7 demonstrates that relative ratios of the temperature factors in all specimens are very consistent and therefore the anisotropy is certainly real.

Extinction coefficient

In the first stages of the refinement, large errors were found in the structure factors of strong low-angle reflections such as 004 (Yosemite forsterite: $F_{\text{obs}} = 98.5$, $F_{\text{calc}} = 130$) or 062 ($F_{\text{obs}} = 90$, $F_{\text{calc}} = 111$). Therefore, a correction for secondary extinction (Zachariasen, 1968) was introduced in the refinement. The extinction coefficient varies by over an order of magnitude (Table 6). It is high for the recrystallized metamorphic forsterites and low for lunar olivines, especially for a crystal from lunar dust (Apollo 11). Extinction from double diffraction is only large for very perfect crystals. We attribute the small extinction in lunar crystals to damage from cosmic and solar radiation. High track densities have been observed in many lunar minerals (e.g., Arrhenius *et al.*, 1971; Comstock *et al.*, 1971; Crozaz *et al.*, 1971; Fleischer *et al.*, 1970, 1971; Price and O'Sullivan, 1970). This type of damage seems more likely than tectonic defects (e.g. by meteorite impact) since asterism and bending is absent in precession photographs. The observation on these four olivines should not be generalized; i.e., the extinction coefficient certainly can not be used to distinguish between lunar and terrestrial olivines. It is quite likely that terrestrial olivine with structural defects also has a small extinction coefficient (Finger, 1969/70). Notice that small extinction coefficients go parallel with large temperature factors, although there is no mathematical correlation between the two parameters. The temperature factor is a function of the Bragg angle and is mainly determined by high-angle reflections. The extinction coefficient is intensity-dependent and affects strong low-angle reflections. Absorption may change the extinction coefficient, although it equally affects strong and weak reflections. There is also no correlation between extinction coefficient and absorption in the four analyzed specimens.

Fe/Mg distribution

Table 6 lists occupancy factors for iron and magnesium on the M(1) and M(2) sites. From these occupancies a distribution coefficient K_D for the reaction $Fe(2) + Mg(1) \rightleftharpoons Mg(2) + Fe(1)$ is calculated,

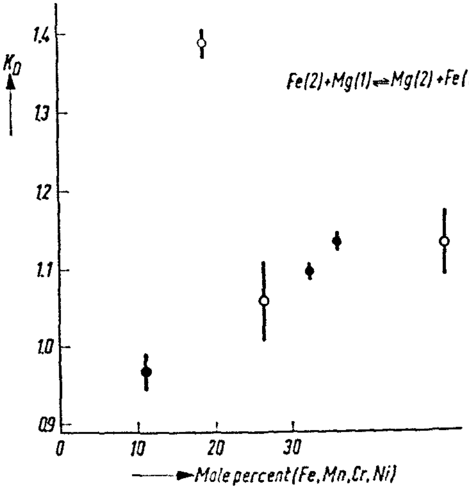

Fig. 3. Fe/Mg distribution coefficient K_D of several Mg-rich olivines as a function of the iron content (error bars are rounded to 1—2 sigmas). $K_D = \frac{Mg(2) \cdot Fe(1)}{Mg(1) \cdot Fe(2)}$.
○ FINGER (1969/70, 1971), ● this paper

and K_D is plotted as a function of the fayalite content in Fig. 3. In metamorphic forsterites, Fe is essentially disordered. In olivines from lunar basalts there is small but significant (over 20 standard deviations) order of iron on the M(1) site. The order of iron is about 5 percent, which is much smaller than 30 percent order, which has been determined from Mössbauer spectra (BUSH *et al.*, 1970; VIRGO *et al.*, 1971). We believe that this small order is real for the following reasons:

1. Errors in the microprobe analyses of the Fe/Mg ratio are about one, at most 2 percent. But the chemical constraint is actually quite insensitive because Fe and Mg occupy the same sites and, regardless of the actual Fe/Mg ratio, the occupancy of the M(1) site in lunar olivines always refined to a heavier electron density of more than twenty standard deviations. Notice that Apollo 11 and 12 crystals gave quite similar results (although in the case of Apollo 12, the Fe/Mg ratio was refined from x-ray data).

2. Standard deviations obtained in the least-squares calculations are real. This is demonstrated for positional parameters by the linear correlation between M—O distances and the fayalite content for the four new data points (Fig. 2) and also by the fact that unit weighting of all reflections (an unrealistic model) shifted the results only 1—2 standard deviations. The latter argument is a good indication of high-quality data. With a perfect data set, the weighting scheme does not affect the results. If a weighting scheme reverses the order relations (Brown, 1971) then the Fe/Mg distribution is beyond the resolution of the refinement or the weighting scheme is wrong.

3. Because of the large difference in scattering factors for Fe and Mg, small errors in the scattering factor table do not change the results appreciably. The same Fe/Mg distribution and the same R value were obtained using neutral or partially ionized atoms. In the present refinement, scale factors for Si and Fe(2) were refined in addition to Fe(1), which determines the Fe/Mg distribution. From these additional scale factors approximate charges have been calculated.

The extremely small Fe/Mg order in olivines suggests that the Fe/Mg distribution does not have a strong thermochemical significance. Order can be only detected satisfactorily in chemically intermediate olivines. These are very rare except in some igneous rocks and therefore the geological importance of Fe/Mg order in olivines is small. Yet we tend to agree with Finger (1969/1970, 1971)—although the present data are not yet conclusive—that in olivines which crystallize from a hot magma (~1200 °C) Fe preferentially occupies the M(1) site. In the metamorphic forsterites, crystallizing at 500—700 °C, order is very small and, if existent, Fe may be enriched on the larger M(2) site.

Electrical charge

The refinement of formal charges affects other parameters insignificantly and barely changes the R value. The results in Table 6 indicate for $Fe = Mg^+ + 0.20$ to 0.30, for Si^+ 0.10 to 0.20, and for O^- 0.10 to 0.20. This is about 5 to 10 percent of the charge of the fully ionized ion. The relatively small actual charge indicates that covalent bonding plays an important role in the olivine structure. We expect that a similar magnitude of formal charges will be found in all silicates and oxides. Because the charges are so small, a good approximation is obtained by applying a constant scale factor to each scattering-factor table for neutral atoms, as discussed above. The refined charges immediately indicate errors in the chemical formula. The value and the standard deviation of the refined charge is a good measure of the resolution of the refinement and will be even more so if we have more data with which to compare it. The introduction of the electrical charge as a variable in the least-squares refinement requires, however, a formal treatment of the various constraints as has been outlined above.

Acknowledgments

H.-R. W. thanks NASA for support through Grants NGR 05-002-414 and NGR 05-003-410, the Miller Institute for Basic Research for a research professorship, and P. B. PRICE for providing the lunar specimens. K. N. R. thanks the NSF for support and the ALFRED P. SLOAN FOUNDATION for a research fellowship. Discussions with G. BROWN, L. W. FINGER, S. GHOSE, S. S. HAFNER, and K. HODGSON are gratefully acknowledged. G. BRIMHALL did the microprobe analyses.

References

G. ARRHENIUS, S. LIANG, D. MACDOUGALL, L. WILKENING, N. BAHANDARI, S. BHAT, D. LAL, G. RAJAGOPALAN, A. S. TAMHANE, V. S. VENKATAVARADAN (1971), The exposure history of the Apollo 12 regolith. Proc. Second Lunar Science Conf. Vol. 3, 2583—2598.

N. V. BELOV, E. N. BELOVA, N. H. ANDRIANOVA, and P. F. SMIRNOVA (1951), Determination of the parameters in the olivine (forsterite) structure with the harmonic three-dimensional synthesis. Dokl. Akad. Nauk SSSR. 81, 399—402.

J. D. BIRLE, G. V. GIBBS, P. B. MOORE, and J. V. SMITH (1968), Crystal structures of natural olivines. Amer. Mineral. 53, 807—824.

L. BORN (1964), Eine „gitterenergetische Verfeinerung“ der freien Mg-Position im Olivin. Neues Jahrb. Mineral., Monatsh. 81—94.

W. L. Bragg und G. B. Brown (1926), Die Struktur des Olivins. Z. Kristallogr. **63**, 538–556.

G. Brown (1971), Order-disorder in olivine. Conf. on petrologic crystal chemistry, AGU. Edgartown, Mass.

R. G. Burns (1969) Evidence for cation ordering in olivine minerals from crystal field spectra (abstract). Acta Crystallogr. A **25**, 559.

R. G. Burns (1970), Crystal field spectra and evidence of cation ordering in olivine minerals. Amer. Mineral. **55**, 1608–1632.

W. R. Bush, S. S. Hafner, and D. Virgo (1970), Some ordering of iron and magnesium at the octahedrally coordinated sites in a magnesium-rich olivine. Nature [London] **227**, 1339–1341.

W. R. Busing, K. O. Martin, and H. A. Levy (1962), ORFLS, a FORTRAN crystallographic function and error program. ORNL-TM-305.

L. G. Caron, R. P. Santoro, and R. E. Newnham (1965), Magnetic structure of $CaMnSiO_4$. J. Physics Chem. Solids **26**, 927–930.

G. M. Comstock, A. O. Evwaraye, R. L. Fleischer, and H. R. Hart, Jr. (1971), The particle track record of lunar soil. Proc. Second Lunar Science Conf. Vol. **3**, 2569–2582.

D. T. Cromer (1965), Anomalous dispersion corrections computed from self-consistent field relativistic Dirac-Slater wave functions. Acta Crystallogr. **18**, 17–23.

D. T. Cromer and J. B. Mann (1968), X-ray scattering factors computed from numerical Hartree-Fock wave functions. Acta Crystallogr. A **24**, 321–324.

G. Crozaz, R. Walker, and D. Woolum (1971), Nuclear track studies of dynamic surface processes on the moon and the constancy of solar activity. Proc. Second Lunar Science Conf. Vol. **3**, 2543–2558.

E. N. Duesler and K. N. Raymond (1971), Conformational effects of intermolecular interactions. The structure of tris-(ethylene diamine) cobalt (III) monohydrogen phosphate nonohydrate. Inorg. Chem. **10**, 1486–1492.

E. N. Eliseev (1958), New data on the crystal structure of olivine. Kristallografiya **3**, 167–175 [Russian]; Soviet Physics–Crystallogr. **3**, 163–170.

L. W. Finger (1967), Determination of cation distribution by least squares refinement of single-crystal x-ray data. Carnegie Institution Year Book **67**, Ann. Report Geophysic. Lab., 216–217.

L. W. Finger (1969/1970), Fe/Mg ordering in olivines. Carnegie Institution Year Book **69**, Ann. Report Geophysic. Lab., 302–305.

L. W. Finger (1971), Fe/Mg ordering in an olivine: a comparison of x-ray and Mössbauer results. Geol. Soc. Amer. abstracts **3**, 310.

R. L. Fleischer, E. L. Haines, H. R. Hart, Jr., R. T. Woods, and G. M. Comstock (1970), The particle track record of the Sea of Tranquillity. Proc. Apollo 11 Lunar Science Conf., Geochim. Cosmochim. Acta, Suppl. 1, Vol. **3**, 2103–2120.

R. L. Fleischer, H. R. Hart, Jr., G. M. Comstock, and A. O. Evwaraye (1971), The particle track record of the Ocean of Storms. Proc. Second Lunar Science Conf., Vol. **3**, 2559–2568.

S. Ghose (1962), The nature of Mg^{+2}–Fe^{+2} distribution in some ferromagnesian silicate minerals. Amer. Mineral. **47**, 388–394.

K. HANKE (1963), Verfeinerung der Kristallstruktur des Fayalits von Bad Harzburg. Neues Jahrb. Mineral., Monatsh. 192—194.

K. HANKE und J. ZEMANN (1963), Verfeinerung der Kirstallstruktur von Olivin. Naturwissenschaften **3**, 91—92.

I. C. JAHANBAGLOO (1969), X-ray diffraction study of olivine solid solution series. Amer. Mineral. **54**, 246—250.

J. L. JAMBOR and C. H. SMITH (1964), Olivine composition determination with small diameter x-ray powder cameras. Mineral. Mag. **33**, 730—741.

H. ONKEN (1965), Verfeinerung der Kristallstruktur von Monticellit. Tschermak's Mineral. Petrogr. Mitt. **10**, 34—44.

P. B. PRICE and D. O'SULLIVAN (1970), Lunar erosion rate and solar flare paleontology. Proc. Apollo 11 Lunar Science Conf. Geochim. Cosmochim. Acta Suppl. 1, Vol. **3**, 2351—2359.

K. N. RAYMOND (1972), The application of constraints to derivatives in least-squares refinement. Acta Crystallogr. A **28**, 163—166.

D. VIRGO, S. S. HAFNER and D. WARBURTON (1971), Cation distribution studies in clinopyroxenes, olivines and feldspars using Mössbauer spectroscopy of ^{57}Fe. Second Lunar Conf. Houston. [Unpublished proceedings].

H. S. YODER and T. G. SAHAMA (1957), Olivine x-ray determinative curve. Amer. Mineral. **42**, 475—490.

W. H. ZACHARIASEN (1968), TeMe: Experimental tests of the general formula. for the integrated intensity of a real crystal. Acta Crystallogr. A **24**, 212